ADA024898

Report No. CG-D-33-76

LOW FRICTION HULL COATINGS FOR ICEBREAKERS: ANALYSIS OF ICEBREAKING IN PARTICULATE ICE

PHASE II, PART III

TECHNICAL REPORT

Document is available to the public through the
National Technical Information Service,
Springfield, Virginia 22151

Prepared for

DEPARTMENT OF TRANSPORTATION
UNITED STATES COAST GUARD
Office of Research and Development
Washington, D.C. 20590

REPRODUCED BY
NATIONAL TECHNICAL
INFORMATION SERVICE
U. S. DEPARTMENT OF COMMERCE
SPRINGFIELD, VA. 22161

17 MAR 1976

The work reported herein was accomplished for the U.S. Coast Guard's Office of Research and Development, Marine Safety Technology Division, as part of its program in Ice Transportation Technology.

The contents of this report reflect the views of Rensselaer Polytechnic Institute, Troy, New York, who are responsible for the facts and the accuracy of the data presented herein. The contents do not necessarily reflect the official views or policy of the Coast Guard. This report does not constitute a standard, specification or regulation.

This document is disseminated under the sponsorship of the U.S. Department of Transportation in the interest of information exchange. The United States Government assumes no liability for the contents or use thereof.

The United States Government does not endorse products or manufacturers. Trade or manufacturer's names appear herein solely because they are considered essential to the object of the report.

W.D. MARKLE, JR., CAPTAIN, USCG
Chief, Marine Safety Technology Division
Office of Research and Development
U.S. Coast Guard Headquarters
Washington, D.C. 20590

TABLE OF CONTENTS

PHASE II - PART III

	Page
BOUNDARY LAYER FLOW OF A NEWTONIAN FLUID SUSPENSION	1
Introduction	1
Analytical Model	1
Equations of Motion for the Multilayered Boundary Layer	3
Velocity Profiles	5
Integral Momentum-Continuity Equations	7
Computations	9
Total Drag Force	11
Results of Newtonian Analysis	13
NOMENCLATURE	14
NON-NEWTONIAN SUSPENSION BOUNDARY LAYER FLOW	16
Introduction	16
Laboratory Model Test	16
Analysis of Model Test	17
Results of Model Tests	29
Analytical Investigation of Drag in Highly Concentrated Fields of Broken Ice	29
Rheological Model	30
Constitutive Equations - Two-Dimensional Bingham Plastic Flow	33
Boundary Layer Solution for Slow Motion of a Bingham Plastic	36
Conclusions and Recommendations	41
REFERENCES	43
NOMENCLATURE	

LIST OF FIGURES

PHASE II - PART III

		Page
Figure III-1	The Development of a Particle-Free Layer (of Thickness δ) in Suspensions of Rigid Spheres	2
Figure III-2	Comparison of Theoretical Viscosity Relationships with Data for Uniform Spheres	3
Figure III-3	.....	4
Figure III-4	Drag Coefficient Constant vs Volume Concentration of Mush Ice	12
Figure III-5	Photograph Showing Crushed Ice Phenomena (Small Particles)	19
Figure III-6	Photograph Showing Crushed Ice Phenomena (Small Particles)	19
Figure III-7	Photograph Showing Crushed Ice Phenomena (Small Particles)	20
Figure III-8	Photograph Showing Crushed Ice Phenomena (Small Particles)	20
Figure III-9	Photograph Showing Crushed Ice Phenomena (Small Particles)	21
Figure III-10	Photograph Showing Crushed Ice Phenomena (Small Particles)	21
Figure III-11	Photograph Showing Ice "Lock Up" (Large Particles)	24
Figure III-12	Photograph Showing Ice "Lock Up" (Large Particles)	24
Figure III-13	Photograph Showing Ice "Lock Up" (Large Particles)	25
Figure III-14	Photograph Showing Ice "Lock Up" (Large Particles)	25
Figure III-15	Photograph Showing Ice "Lock Up" (Large Particles)	26
Figure III-16	Photograph Showing Ice "Lock Up" (Large Particles)	27

Figure III-17 Photograph Showing Ice "Lock Up" (Large Particles) 27

Figure III-18 Photograph Showing Ice "Lock Up" (Large Particles) 28

Figure III-19 Bingham Plastic, Stress-Strain Rate 32

Figure III-20 Region of Plastic Boundary-Layer Flow (Unshaded), with Velocity Profile, in the Moving Plate Problem with $\lambda = 0$ 32

LIST OF TABLES

PHASE II - PART III

Page

Table III-1 9

BOUNDARY LAYER FLOW OF A NEWTONIAN FLUID SUSPENSION

Introduction

In icebreaking one can consider three different modes, ramming, continuous or moving through ice filled water. Several different continuous modes can be identified depending upon the thickness of the ice. Analytical solutions have been attempted and results obtained for the ships resistance in the icebreaking modes, however the role of friction in the resistance of a ship moving in ice filled water is not clear. It has for the most part been ignored. From practical experience it is known that high thrust is needed to move a ship through finely broken ice at low speed. The reason for this is not clear since breaking forces, buoyant forces and momentum interchange would be small. It was proposed that the reason for the high resistance was that the finely divided ice can pack closely together and in essence change the effective viscosity of the water. This is a well known effect of solid fluid mixtures. Accordingly some analytical efforts were instigated to understand ships resistance in ice fields of various density and ice sizes.

Analytical Model

Studies of particulate flows have shown that when a large number of particles are present in a suspension, a particle-free layer soon develops near the wall (Ref.1). The thickness of this region depends on the mean particle concentration c (Fig.III-1). As a result the viscosity of the flow field close to the wall is lower than that of the suspension far from the wall. The same behavior has been observed for nonspherical and spherical particles alike (Ref.2).

Figure III-1a indicates that the time required to establish the equilibrium thickness is of the order of one minute or less for high concentrations.

Figure III-1b shows the relationship between the equilibrium layer thickness δ_∞ and the concentration. The ratio of the particle-free layer thickness to the thickness of the viscous layer can be approximated by the expression

$$c\left(\frac{\delta}{R_o}\right) = 10^{-2}. \qquad (1)$$

The apparent viscosity of suspensions is also a function of the particulate volume concentration. Figure III-2 (Ref.3) shows the effect of particulate concentration on the ratio of the suspension's apparent viscosity to the

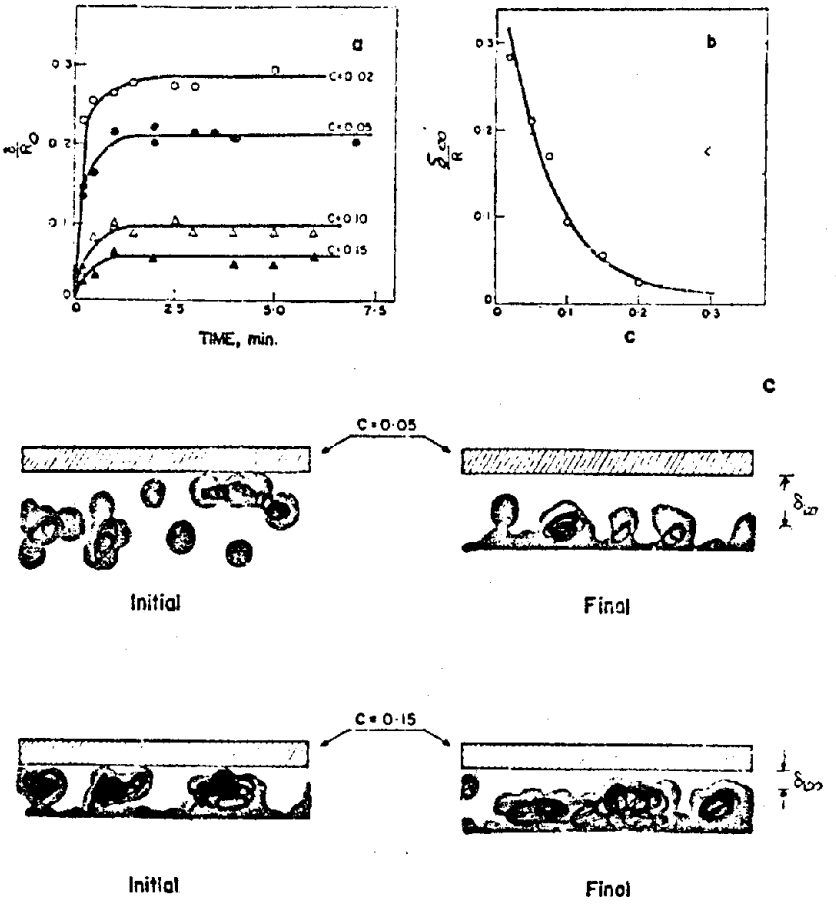

Figure III-1 The Development of a Particle-Free Layer (of Thickness δ) in Suspensions of Rigid Spheres. R = 0.2 cm, a = 0.015 cm (a/R = 0.075), Q = 0.356 cm^3 sec^{-1}.

(a) Variation of δ/R with time. The points are: open circles: c = 0.02; closed circles: c = 0.05; open triangles: c = 0.10; and closed triangles: c = 0.15.

(b) Effect of concentration c on δ_∞/R and δ_∞/a, where δ_∞ is the equilibrium thickness of a particle-free layer attained after a long time.

(c) Tracings from photographs of the particle-free layer for two suspensions. After Karnis, Goldsmith & Mason (1966b).

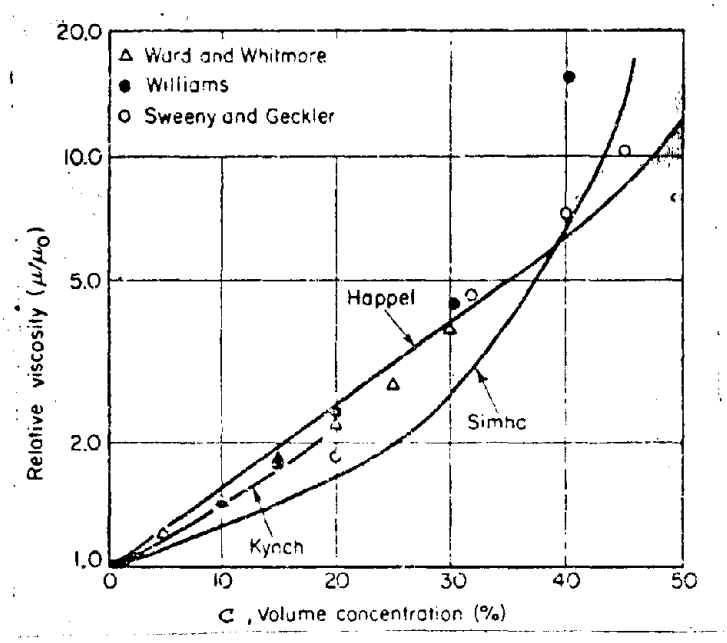

Figure III-2 Comparison of Theoretical Viscosity Relationships with Data for Uniform Spheres

viscosity of the liquid phase alone. Concentrations $c \sim 0.5$ are considered to be about as large as particle packing will permit before the particles come into intimate surface contact with each other. At this limit a tenfold increase in viscosity is observed. The experimental values given in Figure III-2 are accurately correlated by the empirical expression

$$\frac{\mu_v}{\mu} = e^{4.58c} \quad . \tag{2}$$

Equations of Motion for the Multilayered Boundary Layer

Figure III-3 illustrates the problem to be analyzed. The layer next to the boundary of thickness δ is ice-free. The velocity of the interface between the mush ice and the ice-free water is Γ. The integral momentum equation for this layer is

$$\rho \int_0^\delta \frac{\partial}{\partial x} (u^2)\, dy + \rho \Gamma v_\delta = \tau_\delta - \tau_w \tag{3}$$

where τ_w is the shear stress at the wall and τ_δ, the interfacial shear stress at $y = \delta$.

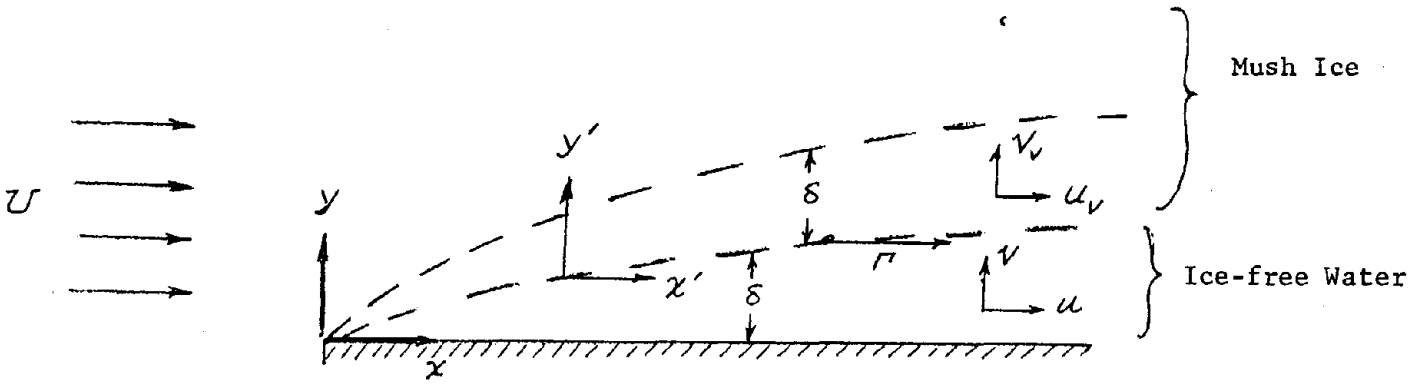

Figure III-3

The integral momentum equation for the mush-ice filled portion of the boundary layer is

$$\rho \int_0^{\delta_v} \frac{\partial}{\partial x} (u_v^2)\, dy' + \rho U v_{v_o} - \rho \Gamma v_{v_\delta} = - \tau_\delta \tag{4}$$

where v_{v_o} is the normal velocity component at the outer edge of the boundary layer and v_{v_δ}, the normal velocity component at the interface.

The normal velocity components at the edges of the boundary layers can be obtained from the continuity equations written for each portion of the boundary layer. The continuity equation for the liquid layer is

$$v_\delta = - \int_0^{\delta} \frac{\partial u}{\partial x}\, dy = v_{v_\delta} . \tag{5}$$

The continuity equation for the ice-filled portion of the boundary layer is

$$\int_0^{\delta} \frac{\partial u_v}{\partial x}\, dy + v_{v_o} - v_{v_\delta} = 0 . \tag{6}$$

Combining Eqs.(5) and (6) yields

$$v_{v_o} = - \int_0^{\delta} \frac{\partial u}{\partial x} dy - \int_0^{\delta_v} \frac{\partial u_v}{\partial y'} dy' . \tag{7}$$

Velocity Profiles

The solution of the preceding integral equations requires the assumption of plausible velocity profiles. These profiles must satisfy the imposed velocity conditions at their extremities and the continuity of shear stress at the ice-free water - mush ice interface.

If a mush-ice profile of the form

$$\frac{u_v}{\Gamma} = a_o + a_1 \eta' + a_2 \eta'^2 \tag{8}$$

is assumed for laminar flow and the following conditions are imposed upon it

$$\frac{u_v}{\Gamma} = \frac{U}{\Gamma} \quad \text{at } \eta' = 1$$

$$\frac{u_v}{\Gamma} = 1 \quad \text{at } \eta' = 0 \tag{9}$$

$$\frac{\partial u_v}{\partial y} = \frac{\partial (u_v/\Gamma)}{\partial \eta'} = 0 \quad \text{at } \eta' = 1$$

then the assumed profile becomes

$$\frac{u_v}{\Gamma} = 1 - 2a_2 \eta' + a_2 \eta'^2 \tag{10}$$

where

$$a_2 = 1 - \frac{U}{\Gamma} = 1 - \frac{1}{R} . \tag{11}$$

The quantity R is the ratio of the interfaced velocity Γ to the free-stream velocity U.

The ice-free liquid velocity near the wall will also be assumed to have a velocity profile of the form

$$\frac{u}{\Gamma} = b_o + b_1 \eta + b_2 \eta^2 . \tag{12}$$

It is required to meet the no-slip conditions

$$\frac{u}{\Gamma} = 0 \quad \text{at } \eta = 0$$
$$\frac{u}{\Gamma} = 1 \quad \text{at } \eta = 1 \tag{13}$$

and also the continuity of shear stress condition at the interface which is

$$\mu_v \left.\frac{\partial u_v}{\partial y'}\right|_0 = \frac{\mu_v \Gamma}{\delta_v} \left.\frac{\partial\left(\frac{u_v}{\Gamma}\right)}{\partial \eta'}\right|_0 = \frac{\mu_v \Gamma}{\delta_v} (-2a_2)$$
$$= \mu \left.\frac{\partial u}{\partial y}\right|_\delta = \frac{\mu\Gamma}{\delta} \left.\frac{\partial\left(\frac{u}{\Gamma}\right)}{\partial \eta}\right|_1 = \frac{\mu\Gamma}{\delta} (b_1 + 2b_2) \ . \tag{14}$$

These conditions lead to a laminar profile of the form

$$\frac{u}{\Gamma} = b_1 \eta + (1 - b_1)\eta^2 \tag{15}$$

where

$$b_1 = 2\left(1 + \frac{\mu_v}{\mu} \frac{\delta}{\delta_v} a_2\right) = 2\left[1 + \frac{F}{G}\left(1 - \frac{1}{R}\right)\right] . \tag{16}$$

The following definitions have been incorporated into the previous equation:

$$\frac{\delta}{\delta_v} = F$$
$$\frac{U}{\Gamma} = \frac{1}{R} \tag{17}$$
$$\frac{\mu_v}{\mu} = \frac{1}{G} \ .$$

The functions F and G are known functions of the mush-ice volume concentration and can be related to Eqs.(1) and (2). For $c > 0.1$, $\frac{\delta}{R_o} < 0.1$, so that $\frac{\delta}{\delta + \delta_v} < 0.1$, or $9 < \frac{\delta_v}{\delta}$. Therefore for $c > 0.1$, Eq.(2) becomes

$$\frac{\delta}{\delta_v} \approx \frac{\delta}{R_o} = \frac{10^{-2}}{c} \ . \tag{18}$$

Comparison of Eqs.(17) and (2) shows that

$$G = e^{-4.58c} . \tag{19}$$

The ratio R will be determined by the equations of motion as a result of the analytical procedures to follow, and is therefore an implicit function of c through its dependence upon F and G.

Integral Momentum-Continuity Equations

When the integral forms of the momentum and continuity equations for the ice-free liquid layer are combined [Eqs.(3) and (5)] the resulting integral equation is

$$\rho\Gamma^2 \frac{d\delta}{dx} \int_0^\delta \frac{u}{\Gamma}\left(1 - \frac{u}{\Gamma}\right) d\eta = \tau_w - \tau_\delta . \tag{20}$$

A similar but more complicated equation is formed when the mush-ice momentum and continuity equations are combined [Eqs.(4) and (6)]

$$\rho\Gamma^2 \frac{d\delta_v}{dx} \int_0^1 \frac{u_v}{\Gamma}\left(\frac{U}{\Gamma} - \frac{u_v}{\Gamma}\right) d\eta' + \rho\Gamma(U - \Gamma) \frac{d\delta}{dx} \int_0^1 \frac{u}{\Gamma} d\eta - \rho\Gamma(U - \Gamma) \frac{d\delta}{dx} = \tau_\delta . \tag{21}$$

In these equations the shear stress terms are given by

$$\tau_\delta = \frac{\mu_v \Gamma}{\delta_v} (-2a_2) \tag{22}$$

$$\tau_w = \frac{\mu\Gamma}{\delta} (b_1) . \tag{23}$$

If it is further assumed that R is independent of x and that

$$\delta = Ax^{\frac{1}{2}} \tag{24}$$

then Eqs.(20) and (21) reduce to, with the aid of Eqs.(22) and (23),

$$\frac{\rho RUA^2}{2} \int_0^1 \frac{u}{\Gamma}\left(1 - \frac{u}{\Gamma}\right) d\eta = \mu b_1 + \frac{2\mu a_2 F}{G} \tag{25}$$

and

$$\frac{\rho RUA^2}{F}\int_0^1 \frac{u_y}{\Gamma}\left(\frac{1}{R} - \frac{u_y}{\Gamma}\right) d\eta' + \rho U(1 - R)A^2 \int_0^1 \frac{u}{\Gamma}\, d\eta - \rho U(1 - R)A^2 = - \frac{2a_2\mu F}{G} . \qquad (26)$$

The integrals which appear in these two equations can be evaluated using the velocity profiles (10) and (15). The assumption that R is a function of c alone and independent of x amounts to a closure of the problem which leads to a similarity solution for the boundary layer thickness, Eq.(24). For the purpose of estimating the effects of the mush-ice viscosity, the presumption that U and Γ bear a fixed relationship to each other depending on the concentration alone does not appear to be overly restrictive.

The various integrals which appear in the latter equations have the following evaluations:

$$\int_0^1 \frac{u}{\Gamma}\, d\eta = \frac{1}{3} + \frac{b_1}{6} \qquad (27)$$

$$\int_0^1 \frac{u}{\Gamma}\left(1 - \frac{u}{\Gamma}\right) d\eta = \frac{2}{15} + \frac{b_1}{15} - \frac{b_1^2}{30} \qquad (28)$$

$$\int_0^1 \frac{u_y}{\Gamma}\left(\frac{1}{R} - \frac{u_y}{\Gamma}\right) d\eta' = - a_2\left(\frac{1}{3} - \frac{2}{15}\, a_2\right). \qquad (29)$$

With these equations (25) and (26) reduce to

$$\rho RUA^2\left[\frac{2}{15} + \frac{b_1}{15} - \frac{b_1^2}{30}\right] = \mu b_1 + \frac{2\mu a_2 F}{G} \qquad (30)$$

$$\rho RUA^2\left[\frac{1}{F}\left(- \frac{1}{3} + \frac{2a_2^2}{15}\right) - \frac{b_1}{6} + \frac{2}{3}\right] = - \frac{2\mu F}{G} . \qquad (31)$$

Eliminating A from the two equations yields

$$\left[b_1 + 2\,\frac{F}{G}\, a_2\right]\left[\frac{1}{F}\left(- \frac{1}{3} + \frac{2a_2}{15}\right) - \frac{b_1}{G} + \frac{2}{3}\right] = - \frac{F}{G}\left[\frac{2}{15} + \frac{b_1}{15} - \frac{b_1^2}{30}\right]. \qquad (32)$$

Since a_2 and b_1 are related through the expression

$$a_2 = \frac{G}{F}\left(\frac{b_1}{2} - 1\right) \tag{33}$$

Eq.(32) can be written in the form

$$b_1^2 + K_1 b + K_0 = 0 \tag{34}$$

where

$$K_1 = \frac{50\ F^2G - 20\ FG - 12\ G^2 + 30\ F^3}{4G^2 - 10\ F^2G - F^3}$$

and

$$K_0 = \frac{4F^3 - 40\ F^2G + 20\ FG + 8G^2}{4G^2 - 10\ F^2G - F^3} \quad . \tag{35}$$

Computations

The values of the most significant parameters will be computed for three values of c = 0.1, 0.3 and 0.5. Table III-1 gives the values of F and G in this range as computed from Eqs.(1) and (2).

TABLE III-1

c	F	G	R	a_2	B
0.1	0.1000	0.6325	0.240	-3.167	0.432
0.3	0.0333	0.2531	0.208	-3.808	0.223
0.5	0.0200	0.1013	0.283	-2.533	0.206

The computed values of b_1 which yield positive values of R are approximately unity for $0.1 < c < 0.5$. This means that the ice-free water velocity profile is essentially a straight line.

The evaluation of b_1 can be facilitated by the accurate approximations

$$K_1 \approx -3 - 5\,\frac{F}{G}$$

$$K_0 \approx 2 + 5\,\frac{F}{G} \quad . \tag{36}$$

Since the coefficient $b_1 \approx 1.0$, the ratio R can be obtained from the expression

$$R = \frac{1}{1 + \frac{G}{F}\left(1 - \frac{b_1}{2}\right)} \approx \frac{1}{1 + \frac{G}{2F}} \quad . \tag{37}$$

Given $a_2 = 1 - \frac{1}{R}$ and $b_1 \approx 1.0$ the value of A can be computed from either Eqs.(30) or (31). An accurate approximation for A is given by

$$A = \sqrt{\frac{6F^2}{GR}\left(\frac{\frac{\mu}{\rho U}}{1 - \frac{2}{5}a_2}\right)} = B\sqrt{\frac{\mu}{\rho U}} \quad . \tag{38}$$

The calculated values of B given in Table III-1 show the expected trend toward a thinner ice-free water layer accompanying the increase in mush-ice concentration. Since R is a function of G/F through Eq.(37) its variation is governed by the nonlinear nature of this ratio as shown in Table III-1. Apparently the interfaced velocity Γ is not strongly influenced by changes in c, remaining roughly 1/4 of the free-stream velocity U over the range of concentrations investigated.

One might envision the role of the ice-free liquid layer next to the wall as essentially a "slip layer" in which the less viscous ice-free water "lubricates" the sliding of the more viscous mush-ice over the solid boundary.

With this in mind a comparison of the wall and interfaced shear stresses is instructive. Their ratio is given by

$$\frac{\tau_\delta}{\tau_w} = \frac{\frac{\mu_v}{\delta_v}\Gamma[-2a_2}{\frac{\mu\Gamma}{\delta}[b_1]} = -2\,\frac{F}{G}\left(\frac{a_2}{b_1}\right) = \left(\frac{2}{b_1} - 1\right) \approx 1.0 \; . \tag{39}$$

Not unexpectedly this liquid layer is little influenced by inertia effects, transmitting the wall shear stress almost undiminished from the wall to the interface. Practically the entire variation in shear stress from τ_w to zero

is accomplished within the mush-ice portion of the boundary layer, and it is here too that the major inertial effects occur.

Total Drag Force

The shear stress at the wall is given by Eq.(23)

$$\tau_w = \frac{\mu R U b_1}{\delta} = \frac{\mu U}{x} \quad \frac{\rho U x}{\mu} \quad \frac{R}{B} b_1 \ . \tag{40}$$

The total drag per unit width of a wall of length L in the flow direction is given by

$$D = \int_0^L \tau_w \, dx = \frac{4 b_1 R}{B} \frac{1}{\frac{\rho U L}{g_o \mu}} \frac{\rho L U^2}{2 g_o} = \frac{K}{\frac{\rho U L}{g_o \mu}} \frac{\rho L U^2}{2 g_o} \tag{41}$$

where

$$K = \frac{4 b_1 R}{B} \approx \frac{4}{F\left(1 + \frac{G}{2F}\right)} \quad \frac{\overline{G\left[1 + \left(\frac{1.5}{1 + \frac{G}{2F}}\right)\right]}}{15} \ . \tag{42}$$

Figure III-4 shows a plot of K as a function of c corresponding to the data given in Table III-1. The value of K is shown extrapolated to the correct limit for the case of completely ice-free flow of $K \cong 1.3$.

The preceding analysis was developed on the basis that the flow was laminar. For ice-free flow this is the situation when the Reynolds number $= \frac{\rho U L}{\mu} < 3.5(10^5)$. If L = 3.0 ft and U = 6 fps = 3.55 kts, $\frac{\rho U L}{\mu} \approx 10.0(10^5)$ which would lead one to conclude that the laminar boundary layer is quite short, which is generally true for single phase flow. It has been shown, however, that turbulence in the free stream greatly influences the transition to turbulent flow within the boundary layer itself. In the case of a ship the free stream is actually at rest while the plate moves relative to it so that free-stream turbulence is negligible. This coupled with the high viscosity of most of the boundary layer and the fact

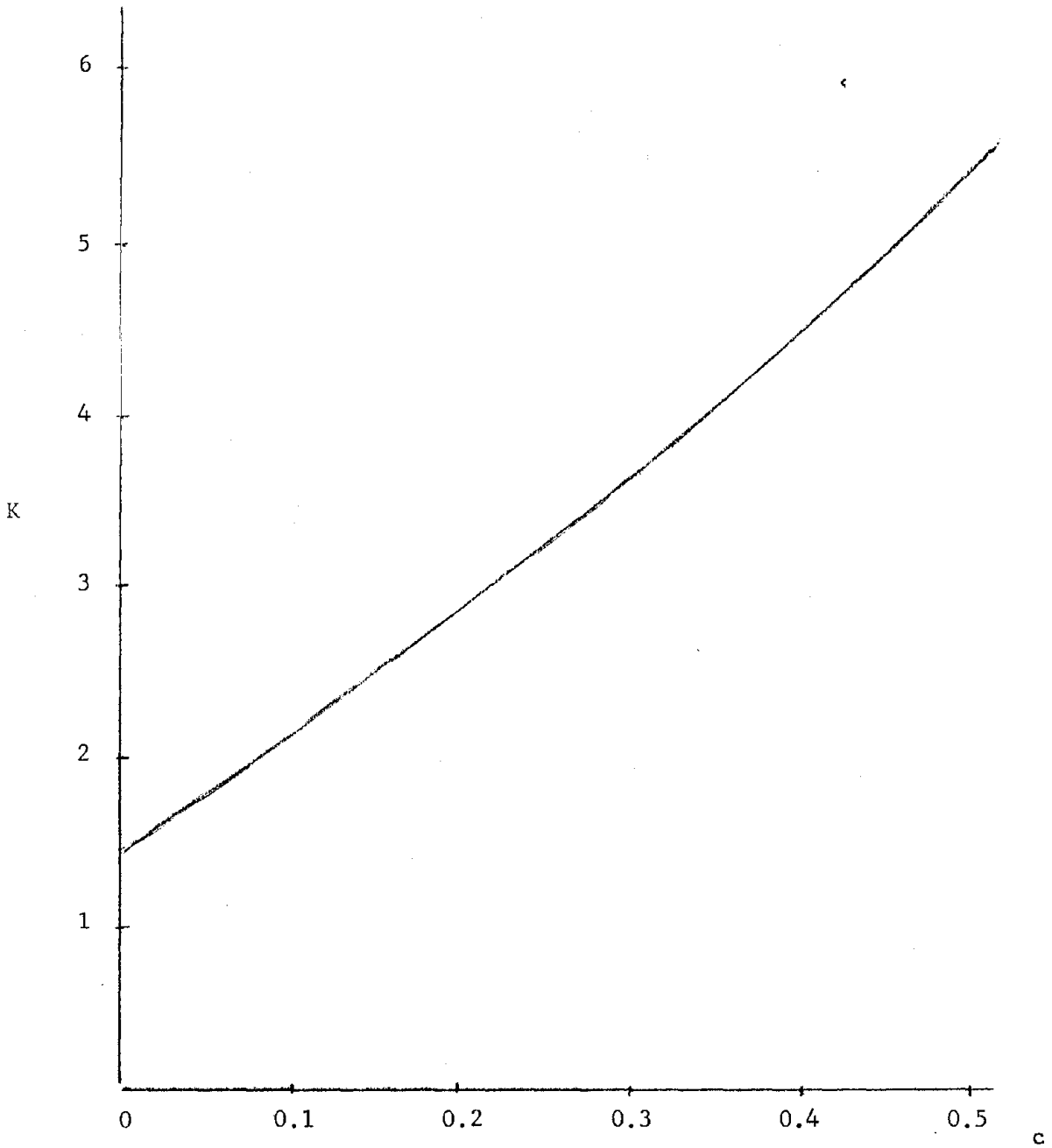

Figure III-4 Drag Coefficient Constant vs Volume Concentration of Mush Ice

that very little water flows into the ice-free region could result in laminarized boundary layer flow at Reynolds numbers well above the normally accepted critical value.

Results of Newtonian Analysis

The effect of a thin layer of ice-free water separating the mush-ice from the wall is to increase the total drag relative to that which is present in the complete absence of floating ice. As expected, this additional drag increases as the volume concentration of the mush-ice increases to its maximum possible concentration. A tenfold increase in the apparent viscosity of the mush ice is accompanied by an approximately four-fold increase in the total drag. This significant increase has obvious implications for bodies moving through ice floes.

NEWTONIAN FLUID SUSPENSION

NOMENCLATURE

A = coefficient, ice-free boundary layer thickness

a = radius of spheres

a_2 = coefficient, mush-ice velocity profile

B = coefficient, ice-free boundary layer thickness

b_1 = coefficient, ice-free velocity profile

c = volume concentration of mush-ice

D = total drag per unit width of plate

$F = \delta/\delta_v$

$G = \mu/\mu_v$

K = coefficient, total drag

K_0 = dimensionless coefficient

K_1 = dimensionless coefficient

Q = volumetric flow rate

$R = \Gamma/V$

R_0 = pipe radius

U = free stream velocity

u = x-component of velocity, ice-free water

v = y-component of velocity, ice-free water

u_v = x'-component of velocity, mush-ice

v_v = y'-component of velocity, mush-ice

v_{v_o} = y'-component of mush-ice velocity at δ_v

$v_{v_o} = v_\delta$ = y'-component of mush-ice velocity at δ

$v_\delta = v_{v_\delta}$ = y'-velocity component at δ, ice-free water

x = coordinate in flow direction, ice-free water

x' = coordinate in flow direction, mush-ice

y = coordinate normal to flow, ice-free water

y' = coordinate normal to flow, mush-ice

Γ = interface velocity

δ = thickness of ice-free water boundary layer

δ_v = thickness of mush-ice boundary layer

$\eta = y/\delta$

$\eta' = y'/\delta_v$

μ = viscosity of ice-free water

μ_v = viscosity of mush-ice

μ_o = viscosity of suspension liquid phase

ρ = density

τ_w = shear stress at wall

τ_δ = shear stress at interface

NON-NEWTONIAN SUSPENSION BOUNDARY LAYER FLOW

Introduction

In the previous section the boundary layer flow of a fluid suspension (in that case water containing floating ice chunks) was as analyzed by treating the mixture as a Newtonian fluid with concentration dependent viscosity. The results obtained from this analysis are applicable to flows in which the volume concentration of broken ice is less than the critical value of about 50%, and the ice chunks are small compared to the characteristic length of the boundary. These conditions could be realized under certain circumstances along the sides of the ship's hull somewhat aft of the bow section. In the vicinity of the bow, however, compacting of the ice by the wedged shape of the bow could be expected to locally increase the concentration of the ice chunks to values exceeding the critical concentration, even if the undisturbed free-field concentrations were initially below the critical value. There is, of course, the possibility that in practice undisturbed free-field concentrations exceeding the critical value will also be encountered, in which case the compacting effect on the ice field by the ship's motion would be much less "localized".

The problem of ship motion in broken ice fields for which the Newtonian, apparent viscosity model is inappropriate is clearly of great interest and worthy of further study. The initial considerations of this difficult and apparently almost neglected problem will be the subject of the remainder of this report.

Laboratory Model Test

Before attempting any analytical investigation of highly concentrated ice-water suspensions it was decided that it would be helpful if the behavior of such mixtures was modeled and observed in the laboratory. A simple demonstration apparatus was therefore devised. The purpose of this experiment was to

investigate some of the properties of ice and water and the effects of moving a boat through broken ice. The apparatus used consisted of a large tub 5' by 2' by 5" deep-filled halfway with water and two small boats, the shorter made of plastic, the longer of wood.

The first experiments were done using crushed ice. In order to get the water in the tub cooled down ice cubes were first allowed to melt in the water and then the crushed ice was added. One of the boats was then be placed at one end of the tank and moved slowly through the ice.

Analysis of Model Test

Instead of the boat moving from one end of the tank to the other, breaking through the ice, it was found that the ice would move in around the boat, interlocking to form an ice sheet, following which the entire ice field would move with the boat. Even ice originally behind the boat would cling to other pieces of ice and move along so that the boat was not only pushing the ice field in front of it but pulling the one in back of it too. It appeared as if all the tiny particles of ice had frozen together. This was not the case, however, since when the field was poked with a finger all the particles easily separated showing that the chunks had not frozen together.

If, as the boat was moving, a portion of the ice field to the side of the boat was broken off by running a finger through the field perpendicular to the side of the boat, this separated part of the ice field would remain as a sheet of ice and move in behind the boat once it had passed by.

With the crushed ice there was never any difficulty reproducing these phenomena. The best results were obtained with a water temperature between 33°F (0-2°C) and 38°F and a surface density of 60% or 70% ice to water. The same effects were obtained with a surface density of ice to water as low as 50%. Some wall

effects were encountered during the tests. If the ice was moved away from the wall at the beginning of the boat's run, it would form the ice sheet and then once again be forced against the wall by the motion of the boat.

The pictures on the following pages illustrate the phenomena described above for crushed, tiny particle ice. The ice cubes in these photographs are what remained of the original cubes after cooling down the water. The smaller pieces were subsequently added as crushed ice. The black spot in some pictures are on the bottom of the tub and therefore show holes in the ice field.

Figures III-5, III-6, III-7 - In these pictures the boat started moving from the end of the tank. It carried with it the entire field of ice. This can be seen by noticing the perpendicular line directly behind the boat, indicating the end of the ice field. The blur at the bottom of the picture is the ice crushing against the opposite wall.

Figure III-8 - In this picture the boat was placed in the center of the field and then started moving. It carried with it the field in front of it and the field in back of it. The arrow points to the line made by the moving field showing clearly how the entire field moves.

Figures III-9 and III-10 - Here the boat started moving at the end of the tank carrying the entire field. A portion of the field was broken off by running a finger through the field perpendicular to the side of the boat. One can see that as the boat moves forward still carrying the field, this separated portion moves in behind the boat. The black spots are on the bottom of the tank. They show where there are holes in the field. The field still moves even with the presence of a large number of holes.

Figure III-5

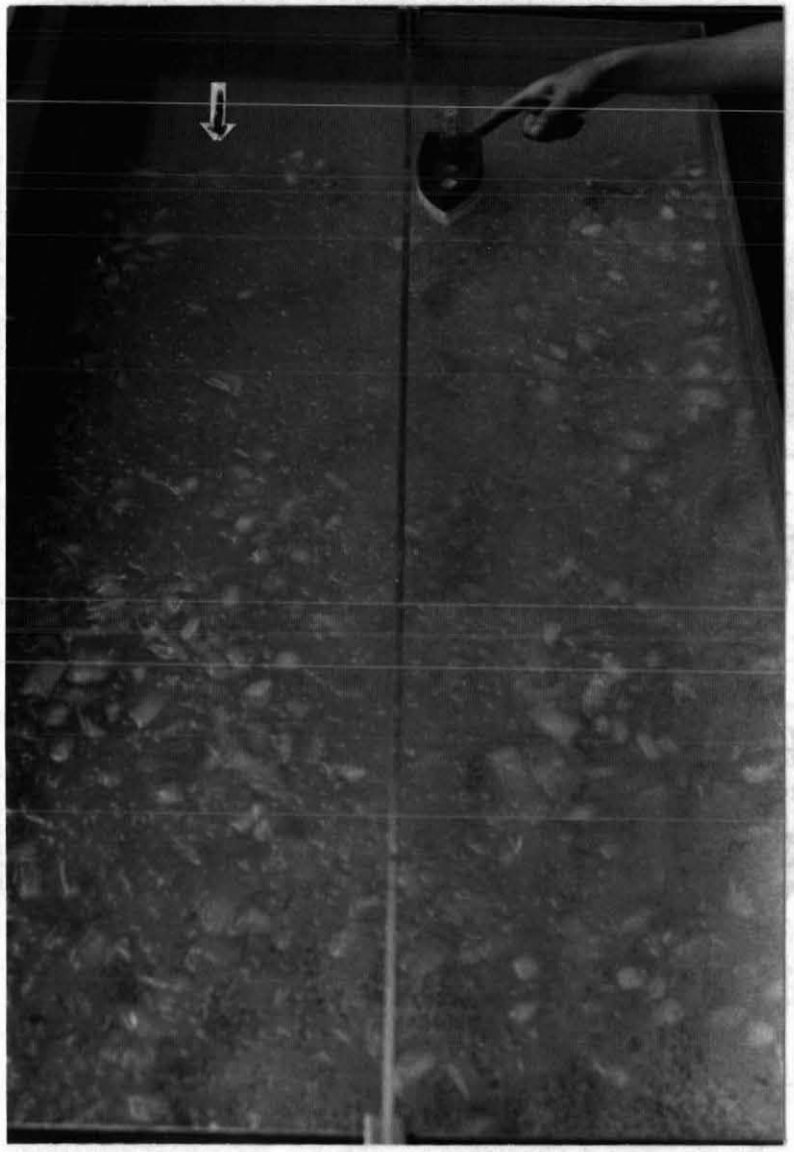

Figure III-6

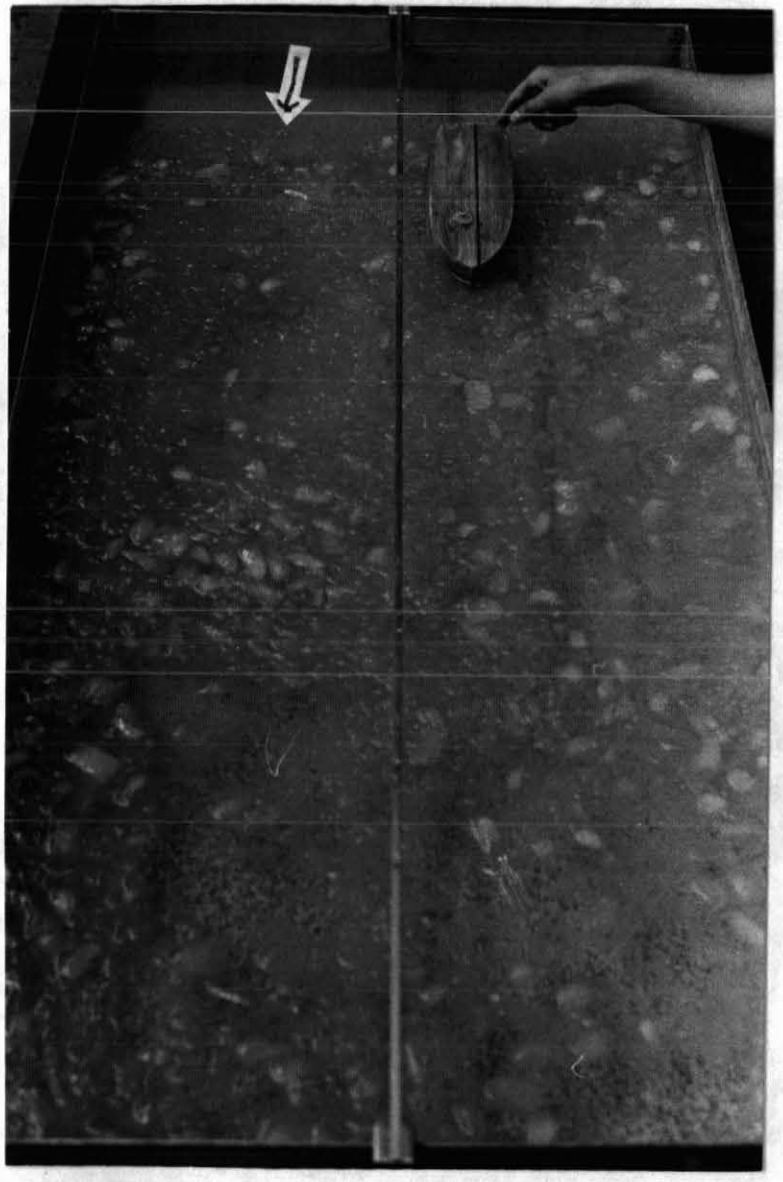

Figure III-7

Figure III-8

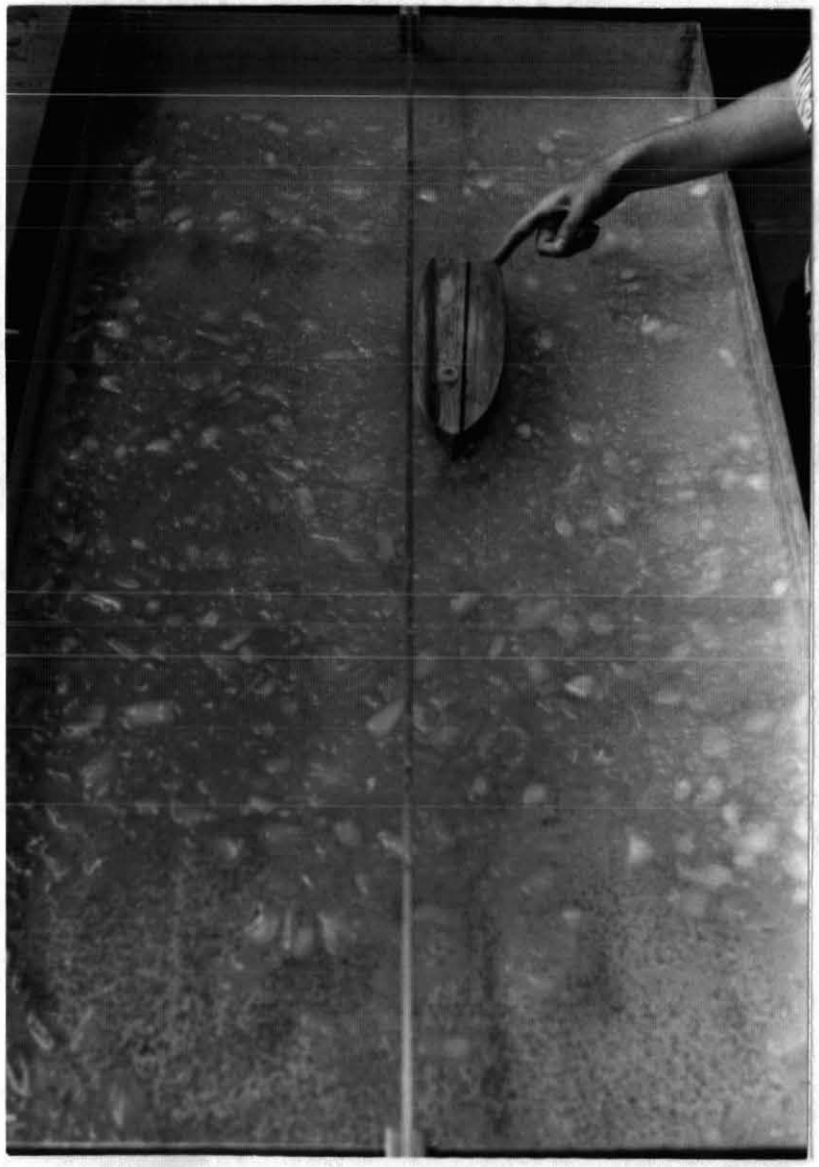

Figure III-9

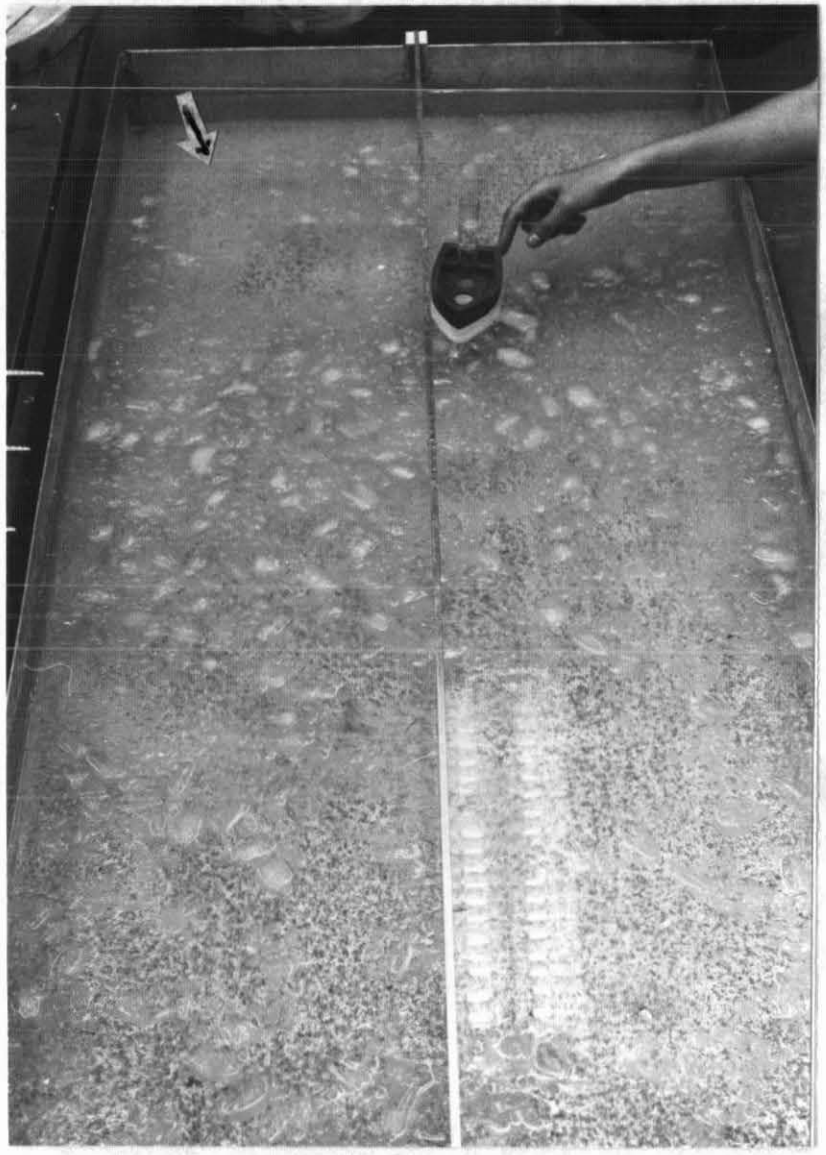

Figure III-10

The crushed ice particle results looked almost identical for the two different shaped boats. Unfortunately, very few details or specific properties of the ice-water flow could be identified using such small particles. When intermediate size ice cubes were used, however, much more could be seen and the results began to make some sense. Photographs of actual icebreakers in broken ice show that there are about 50 - 100 pieces of ice to the length of the boat. This makes the crushed ice experiments somewhat more realistic than the ones using ice cubes 7 - 15 pieces to the length of the boat.

With these larger chunks of ice one could easily see the "lock-up" of all the ice. Once again they appeared to be frozen together but when poked the cubes would separate. Even without the boat in the tub the ice would seem to lock-up when a wave in the water was created.

One of the first things investigated was whether or not the particle size had an influence, i.e., is there a particle size above which the boat will not push the whole ice field? To test for this effect, full size ice cubes were initially placed in the tub. As the cubes melted the boat was passed through the field of smaller and smaller ice chunks. It was concluded that if the water was cold enough (around 33°F - 34°F) and if the cubes were in the water long enough to begin melting, the particle size was of no importance. When the water was cold and full size cubes were added there was no effect at first, but given a minute or two to begin melting, the ice field could easily be moved by either boat. Perhaps this melting creates a new coefficient of friction or some new resistance between the ice and the water.

In order to find the conditions which determined whether the boat would carry the field or just break through the ice, the boat was watched carefully as it began moving. It was observed that under the correct conditions (cold

water and no wall effect present) if the boat submerged a cube in front of it, then it would begin to move the whole field. This action was easily identified because at this point a small extra force would be needed to keep the boat moving forward. If the boat were moved away just enough to allow the submerged cube to come up, when the boat was moved ahead again it would begin breaking through the ice. Apparently there must be a submerged cube present to cause the boat to move the field.

Again, as with the crushed ice, the boat was able to move the field to its side and behind. If, as before, a portion of the field was broken off to the side, it would move in behind the boat remaining locked up.

Figures III-11 and III-12 - One can clearly see the arrangement of the ice when it is all "locked up". The boats both started at the end of the tank and have carried the field with them.

Figures III-13 and III-14 - After the boat has moved some distance within the ice field, portions of the field were cut away along a line running through the ice perpendicular to the side of the boat. Then as the boat moved forward these sections remained "locked up" and moved in behind the boat.

Figure III-15 - Here one can see that even with the larger cubes the boat can carry with it parts of the ice field that have formed behind it.

Figures III-16 and III-17 - These are close-ups of the boat in the ice field. The arrow in Figure III-17 points to the cube that has been submerged.

Figure III-18 - The boat has been moved away but the "locked up" ice field can still be seen. The finger points at the cube that has a submerged cube under it. The arrow points at the submerged cube itself.

Figure III-11

Figure III-12

Figure III-13

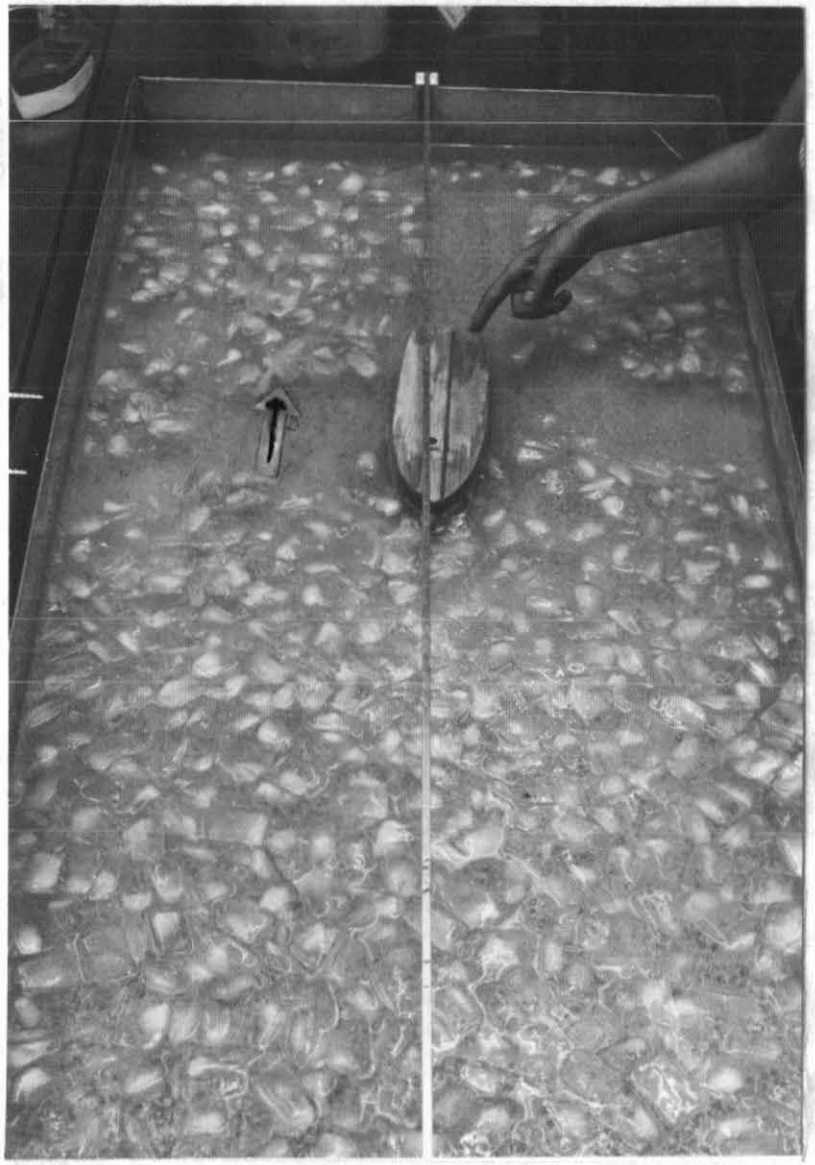

Figure III-14

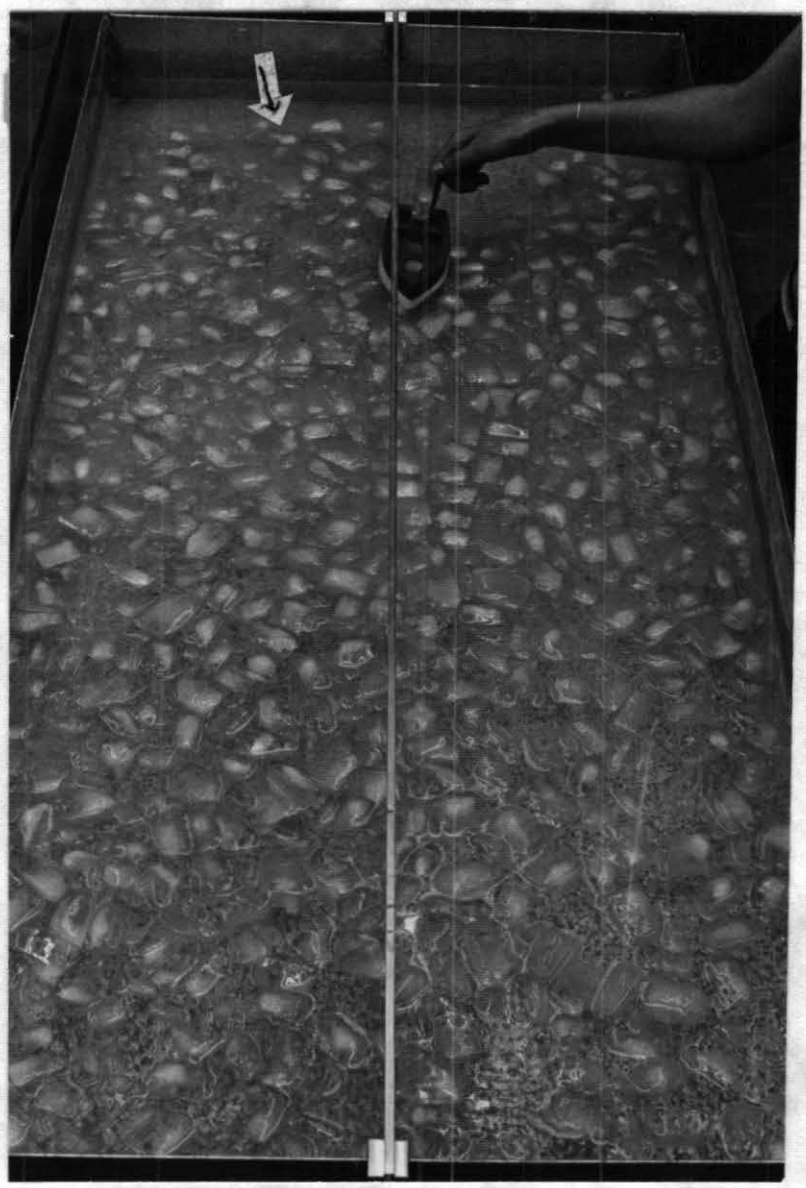

Figure III-15

Figure III-16

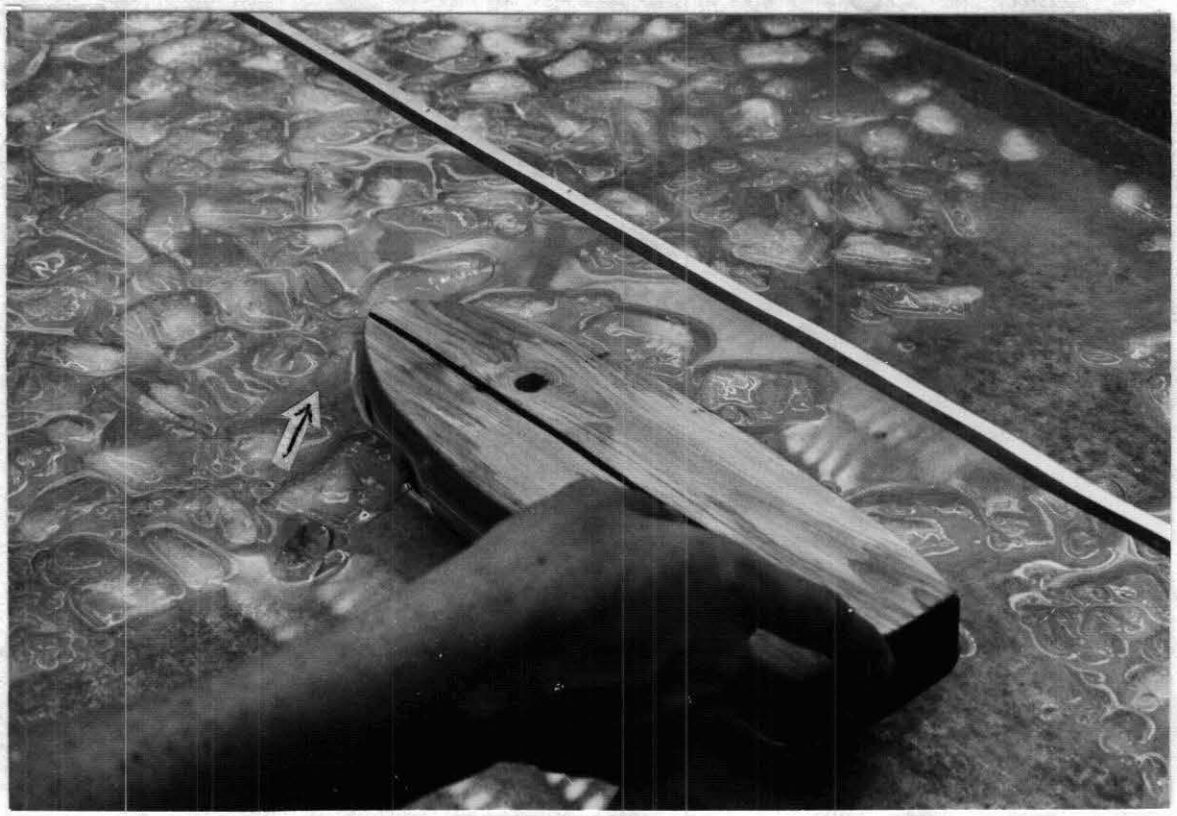

Figure III-17

Figure III-18

Results of Model Tests

The large cubes probably do not give a totally realistic view of what would happen in a full-scale ice field. However, they do allow us to view what we cannot see with the smaller crushed ice particles. If these results can be scaled up to a full size icebreaker, they would indicate that icebreakers try to drag entire ice fields with them. If the ice is in the process of melting, the boat must move the whole ice field. The particle size, whether all large, all small, or mixed, does not seem to matter.

It may be of some significance to mention that the longer boat seemed to be able to submerge cubes easier than the shorter boat and was therefore more likely to move the entire ice field. Since broken off portions of the ice field did move in behind the boat, maybe this accounts for the icebreakers getting stuck and not being able to back out.

In these experiments no effort was made to keep the boats from dragging ice fields. No data has been taken to measure the forces on the boats.

Although the extent of the "locked up" ice field shown here may be exaggerated relative to full-scale behavior, these tests do indicate that there is a tendency of floating particulate material to interact in such a way as to cause large coalesced regions to move as a unit.

Analytical Investigation of Drag in Highly Concentrated Fields of Broken Ice

In the previous analysis the drag of a fluid containing a low concentration of suspended, broken ice particles was investigated. In that case it was assumed that the presence of particulate ice would cause the suspension's apparent viscosity to increase depending on the concentration of the ice particles. It was demonstrated that under these conditions the drag on a flat plate could be substantially increased as a result of the ice particles in the suspension.

This earlier analysis was necessarily limited to suspensions whose ice particle concentration is sufficiently small, that they experience little or no particle-to-particle interference. Such fluids do not tend to become "structured" in the sense that a solid is since the particles do not frequently come into contact, but influence each others motion only through the action of the intervening liquid. In this section a model for highly concentrated ice-water suspensions which do tend to become structured will be proposed and then used to obtain the characteristics of the flat plate boundary layer flow for such a fluid.

Rheological Model

The rheological properties of highly concentrated suspensions of ice and water do not seem to have been investigated either in the laboratory or the field. However, even a casual observation such as described above of the response of concentrated suspensions to the motion of bodies through them indicates that they cannot be treated as Newtonian fluids. Apparently the particle-to-particle interference caused by high particulate concentrations causes certain portions of the ice field to behave more like a solid than a fluid. This effect is undoubtedly caused by the consolidation of the floating particulate into a loosely interlocking matrix in which the water phase plays a minor role as the lubricant.

Since a direct experimentally determined characterization of the stress-strain relationship for broken ice fields does not seem to be available at this time it was decided to look for an analogous flow field whose properties are known and then to model the water-ice suspension after it. The most logical analogous flow is that which occurs in fluidized beds. Here the particulate material is suspended in an upward moving fluid stream rather than by buoyancy

forces. Particle-to-particle interaction plays an important role in the performance of these beds and so it is a matter of some concern to those who use them. Of the considerable literature on the subject of fluidized beds two references proved to be of particular interest with regard to broken ice fields (Refs.4,7). In both these references it was demonstrated experimentally that highly concentrated particle-fluid suspensions exhibit non-Newtonian behavior to a degree depending on the concentration of the particulate material.

These suspensions are found to require that a minimum shear stress be exerted upon them before they will yield continuously in the manner of a fluid. In Ref.4, which is most applicable to the problem at hand, it was shown that the stress-strain relationship for a suspension undergoing pure shear follows very closely the classical constitutive equation for a Bingham plastic. A Bingham plastic (Fig.III-19) is a material which will not yield until a minimum shear stress is exceeded, and then once deformation does begin it follows a linear stress-strain rate relationship similar to a Newtonian fluid. This Bingham plastic-like behavior was particularly representative of those suspensions which contained the larger size particles.

It could certainly be argued that for shear rate as small as 1.0 sec^{-1}, which are typical for ships, any suspension requiring a minimum shear stress could be considered to be a Bingham plastic. The Bingham plastic constitutive equation also happens to be one of the simpler non-Newtonian formulations, thereby lending itself to analytical techniques.

Thus, based on observations of the behavior of an analogous material and the relative simplicity of its constitutive equation, it was assumed as a first approximation that highly concentrated ice-water suspension obey the constitutive equations for a Bingham plastic in the range of shear rates encountered in ship motion. The actual confirmation of the Bingham model and the determination

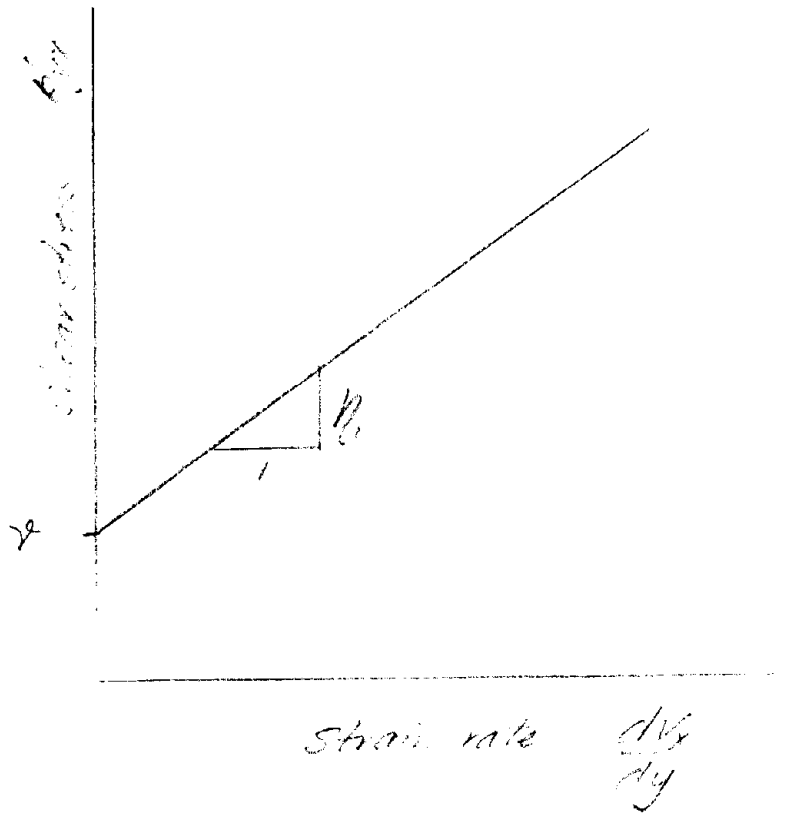

Figure III-19 Bingham Plastic, Stress-Strain Rate

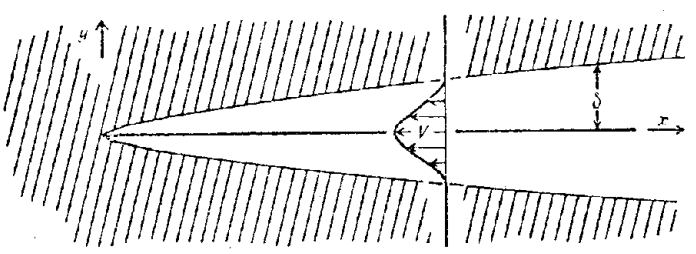

Figure III-20 Region of Plastic Boundary-Layer Flow (Unshaded), with Velocity Profile, in the Moving Plate Problem with $\lambda = 0$. The vertical scale is much increased compared with the horizontal.

of its two material coefficients must necessarily be left for laboratory confirmation at some later date. There is strong evidence from Refs.4 and 7 that these coefficients will depend on the size, distribution and concentration of the particulate ice. There is little doubt, however, that these suspensions can be characterized as Bingham over some range of shear rates in the neighborhood of zero once the shear rate-stress relationship is found from rheological measurements.

Constitutive Equations - Two-Dimensional Bingham Plastic Flow

For one-dimensional flows the equation relating the shear stress to the strain rate (see Fig.III-19) can be expressed by the equations

$$p'_{yx} = \left(\eta_1 + \frac{\nu}{\left|\frac{dv_x}{dy}\right|}\right)\frac{dv_x}{dy} \; ; \; |p'_{yx}| > \nu$$
$$\frac{dv_x}{dy} = 0 \; ; \; |p'_{yx}| < \nu \; . \tag{43}$$

There are an infinite number of ways which this special case formulation can be generalized to two and three-dimensional flows. The most common generalization used is that proposed by von Mises. His equations are summarized in Ref.8 and are as follows:

$$p_{jj} = 3K\Delta \tag{44}$$

$$p'_{ik} = 2\mu\epsilon'_{ik} \; ; \; \frac{1}{2}\,(p'_{ik}p'_{ik}) \le \nu^2, \text{ elastic} \tag{45}$$

$$p'_{ik} = 2\eta\epsilon'_{ik} \; ; \; \frac{1}{2}\,(p'_{ik}p'_{ik}) > \nu^2, \text{ plastic} \; . \tag{46}$$

In the first equation K is the bulk modulus of the material. Since the pressure is defined as $p = -\frac{1}{3}\,p_{jj}$ and Δ = dilatation = the change in volume per unit volume, the first equation states that the pressure is related to the change in volume of a unit volume by the bulk modulus.

The components of the strain tensor are given by

$$\epsilon_{ij} = \frac{1}{2}\left(\frac{\partial u_i}{\partial x_j} + \frac{\partial u_j}{\partial x_i}\right)$$

where u_i are the components of the displacement. The dilatation is given by

$$\Delta = \epsilon_{jj} .$$

The second equation applies in the elastic region where the material is deformed but where the deformation rate $\dot{u}_i = 0$. The modulus of rigidity is given the symbol μ. If the stress components are separated into two parts so that p'_{ik} are the deviatoric components, then the total stresses are given by

$$p_{ik} = p'_{ik} - p\delta_{ik}$$

where δ_{ik} is the substitution tensor.

The deviatoric components of the elastic stress tensor (which are related to the modulus of rigidity) are related to the components of the elastic strain tensor by the second equation. This equation is the standard constitutive equation of linear elasticity in which the normal components contain the effects of the hydrostatic pressure p. This equation can also be written in the form

$$p_{ik} = -p\delta_{ik} + \mu\left(\frac{\partial u_i}{\partial x_k} + \frac{\partial u_k}{\partial x_i}\right) . \tag{45}$$

Equation (45) applies only if a minimum state of stress ν is not exceeded so that

$$\frac{1}{2}\, p'_{ik} p'_{ik} \leq \nu^2 .$$

This limiting condition will be discussed more thoroughly in a succeeding paragraph.

The third equation expresses the fact that the material will yield in a viscous fashion once the critical stress condition ν has been exceeded. The

flow in this regime is analogous to the flow of a viscous fluid where η is the viscosity (variable in this case) and

$$e_{ij} = \frac{1}{2}\left(\frac{\partial \dot{u}_i}{\partial x_j} + \frac{\partial \dot{u}_j}{\partial x_i}\right) = \dot{\varepsilon}_{ij} .$$

The quantities $\dot{u}_i$ are the velocity components of the flow field.

One more equation is needed in addition to the first three, and that is the equation for the variable viscosity, comparable to that which appears in Eq.(42). The generalization proposed by von Mises is

$$\eta = \eta_1 + \frac{\nu}{\sqrt{2e'_{ik}e'_{ik}}} . \tag{47}$$

This form of the variable viscosity reduces to the form of Eq.(42) for one-dimensional flow and contains two material coefficients, the yield value and the reciprocal mobility η_1. These are the two quantities mentioned earlier which must be obtained experimentally.

An equivalent form of the apparent viscosity equation (47) is

$$\eta = \frac{\eta_1}{1 - \dfrac{\nu}{\sqrt{\frac{1}{2}\, p'_{ik}p'_{ik}}}} .$$

Here it can be seen that as $\frac{1}{2}\, p'_{ik}p'_{ik} \rightarrow \nu^2$ the apparent viscosity approaches infinity as indicated in Fig.III-19 for one-dimensional flows. It can be easily shown that $p'_{ik}p'_{ik}$ is invariant under coordinate rotation so that the apparent viscosity is a proper scalar. On the other hand $p'_{ik}p'_{ik}$ can vary from point to point in the material so that similar to the one-dimensional case the apparent viscosity in Eq.(4) also varies from point to point. Since $\sqrt{e'_{ik}e'_{ik}} \neq e'_{ik}$ the generalized three-dimensional model is further complicated by the fact that the variable viscosity does not simplify as neatly as the one-dimensional version.

Boundary Layer Solution for Slow Motion of a Bingham Plastic

Obviously the analytical solution of a two-dimensional flow around a body shaped like the hull of a ship is a difficult task even when the fluid is Newtonian. The added complication of a variable viscosity, which itself depends on the kinematics or state of stress within the flow field, probably precludes the possibility of finding an analytical solution for flows around two-dimensional bodies except through the use of a computer.

Fortunately Oldroyd (Ref.9) has investigated a problem which has some bearing on the one at hand. The results of his analysis will be described here since they reveal some of the salient features of the flow produced by bodies moving through two-dimensional fields of Bingham fluids.

In this analysis the elastic regions will be treated as essentially rigid. In this way the elastic regions enter into the picture only as boundary conditions at surfaces of transition from elastic to plastic states along what could be called a yield surface. In the plastic region the flow will be assumed to be incompressible so that

$$\frac{\partial v_i}{\partial x_i} = 0$$

where $v_i = \dot{u}_i$. The components of the strain-rate tensor for the plastic region are given by

$$e'_{ik} = \frac{1}{2}\left(\frac{\partial v_i}{\partial x_j} + \frac{\partial v_j}{\partial x_i}\right) .$$

For two-dimensional flows the stream function is defined by

$$u = -\frac{\partial x}{\partial y} , \quad v = \frac{\partial y}{\partial x}$$

so that

$$e'_{xx} = -\frac{\partial^2 \psi}{\partial x \partial y} , \quad e'_{yy} = \frac{\partial^2 \psi}{\partial x \partial y}$$

$$e'_{xy} = \frac{1}{2}\left(\frac{\partial^2 \psi}{\partial x^2} - \frac{\partial^2 \psi}{\partial y^2}\right) .$$

Starting with equations of motion

$$\rho \frac{Dv_i}{Dt} = - \frac{\partial p}{\partial x_i} + \frac{\partial p_{ki}}{\partial x_k} \quad .$$

Oldroyd develops plastic boundary layer equations of the form

$$\frac{\partial p}{\partial x} = \eta_1 \frac{\partial^2 u}{\partial y^2} + 2\nu\left\{\frac{\partial}{\partial x}\left(\frac{\partial u}{\partial x} / \frac{\partial u}{\partial y}\right) - \frac{\partial}{\partial y}\left(\frac{\partial u}{\partial x} / \frac{\partial u}{\partial y}\right)\right\} \tag{48}$$

$$\frac{\partial p}{\partial y} = - 2\nu \frac{\partial}{\partial y}\left(\frac{\partial u}{\partial x} / \frac{\partial u}{\partial y}\right) \tag{49}$$

on the assumption that

$$\frac{1}{\left(\frac{\nu d}{\eta_1 v}\right)^{2/3}} \ll 1.0$$

and

$$\frac{\rho V d}{\eta_1} \sim 1.0$$

where d And V are the characteristic length and velocity of the flow field.

Equations (48) and (49) are the equations for the two-dimensional creeping flow of a Bingham fluid in which all inertia terms are absent and only the largest stress related terms remain.

These equations were applied by Oldroyd to the solution of the plastic boundary layer near the semi-infinite thin plate shown in Fig.III-20. In this problem the thin plate moves with a velocity V to the left through an infinite mass of a Bingham fluid which itself has zero velocity where undisturbed.

Equations (48) and (40) apply in the region $0 \leq y \leq \delta(x)$, i.e., the so-called boundary layer. The boundary conditions for the flow in this region are

$$u = -V, \; v = 0 \quad \text{on } y = 0$$

$$u = V = 0, \; \frac{\partial u}{\partial y} = 0 \quad \text{on } y = \delta(x). \tag{50}$$

An additional boundary condition must be imposed at the edge of the boundary layer describing the pressure exerted by the external elastic region on the

edge of the boundary layer itself. This pressure will depend on the stress distribution in the elastic region. As a first approximation it will be assumed that the pressure is a constant, so that

$$p = p_1 \text{ (constant) on } y = \delta(x) \ . \tag{51}$$

The significance of this assumption with respect to icebreaking will be discussed later.

The details of the solutions of Eqs.(48) and (49) using conditions (50) and (51) are given in Ref.9 and will not be repeated here. The results of the solution are as follows:

$$p - p_1 = -4\nu\left(\frac{\eta_1 V}{2\nu x}\right)^{1/3} (1 - Y \tag{52}$$

$$u = -V(1 + 2Y)(1 - Y)^2 \tag{53}$$

$$v = V\left(\frac{\eta_1 V}{2\nu x}\right)^{1/3} (4Y^3 - 3Y^4) \tag{54}$$

where

$$Y = \frac{y}{3x}\left(\frac{2\nu x}{\eta_1 V}\right)^{1/3} \tag{55}$$

and

$$\delta(x) = 3x\left(\frac{\eta_1 V}{2\nu x}\right)^{1/3} \ . \tag{56}$$

This solution suffers from the same deficiencies as all boundary layer solutions. As usual the boundary condition $v = 0$ on $y = \delta(x)$ is not satisfied exactly. However, for large values of $\frac{\nu x}{\eta_1 V}$ this condition is very closely approximated since

$$v(\delta) = V\left(\frac{\eta_1 V}{2\nu x}\right)^{1/3} \ .$$

The above solutions are also unreliable approximations very near the plate's leading edge where the boundary layer approximations are always inaccurate. The region of the flow field in which the approximations fail are fortunately quite small, and generally do not prove to be troublesome if one is only interested in the global features of the flow such as the total drag on the whole plate.

A curious feature of this flow field solution is the fact that the velocity profile in the boundary layer yields

$$\left.\frac{\partial u}{\partial y}\right|_{y=0} = 0$$

so that the shear stress on the boundary is simply ν and the total drag on the plate (both sides) is 2ν times the area of the plate (one side). This result is a consequence of the assumption of slow flow. It also suggests a means by which the material coefficient ν might actually be measured in the laboratory.

Although the flow around a thin plate does not model the flow around the hull of a ship it at least indicates the nature of the effects which the rheology of the material has on the drag. For this simple configuration we find that the drag is dependent upon a property of the suspension ν, the area of the surface, and independent of the normal stress and the velocity of the plate. This leads to a friction law of the type $F \propto \nu \times$ area which applies once motion occurs. To initiate the motion from rest one must, of course, apply a force equal to $\nu \times$ area otherwise the entire ice-water field is deformed elastically while the plate displaces only slightly as it loads the field. The frictional behavior here is analogous to the Coulomb friction case where sliding is initiated only if a certain minimum tangential force is applied.

The "sticking effect" caused by ν has particular significance for ship hulls since it indicates that a certain minimum thrust must be exerted by the propellers to set the ship in motion when it is at rest in a concentrated broken ice-water field. This is contrary to the behavior expected in less concentrated broken ice fields where even the slightest thrust will set the ship into motion through the Newtonian fluid.

The solutions given above suffer from one other deficiency and that is the fact that the pressure on the plate is found to be less than the pressure in

the free stream. When Eq.(52) is evaluated at y = 0 the pressure on the plate is given by

$$p - p_1 = -4\nu\left(\frac{\eta_1 V}{2\nu x}\right)^{1/3} .$$

This means that the free surface of the fluid would tend to sink down as the plate surface is approached. This is certainly contrary to the observed behavior along two-dimensional bodies where there is a definite "ridging" upward of the ice, especially near the leading edge. Oldroyd (Ref.9) shows that another pressure boundary condition at the edge of the boundary layer is admissible which is

$$p = p_1 + p_2(x) \quad \text{on } y = \delta(x) \tag{57}$$

where

$$p_2 = 2\lambda\nu \frac{d\delta}{dx}$$

λ = a dimensionless constant.

With this modification the previous solutions are amended to read:

$$\delta(x) = 3x\left(\frac{\eta_1 V}{2(1+3\lambda)\nu x}\right)^{1/3} \tag{58}$$

$$p - p_1 = -4\nu\left(\frac{\eta_1 V}{2(1+3\lambda)\nu x}\right)^{1/3}(1 - \lambda - Y) \tag{59}$$

$$u = -\frac{V(1+3\lambda+2Y)(1-Y)^2}{1+3\lambda} \tag{60}$$

$$v = \frac{V}{1+3\lambda}\left(\frac{\eta_1 V}{2(1+3\lambda)\nu x}\right)^{1/3}\{4Y^3 - 3Y^4 + \lambda(6Y^2 - 4Y^3)\} \tag{61}$$

$$Y = \frac{y}{3x}\left(\frac{2(1+3\lambda)\nu x}{\eta_1 V}\right)^{1/3} . \tag{62}$$

The condition that $\frac{\partial u}{\partial y}$ and $\delta(x)$ are positive requires λ to be a positive number.

The total drag on the plate (both sides) in this case now becomes

$$F = 2\nu\ell\left\{1 + 12\lambda\left(\frac{\eta_1 V}{2(1+3\lambda)\nu\ell}\right)^{2/3}\right\} . \tag{63}$$

Under these circumstances the value of $p_2(x)$ at the outer edge of the boundary layer is given by

$$p_2(x) = 4\lambda\nu\left(\frac{\eta_1 V}{2(1+3\lambda)\nu x}\right)^{1/3} . \tag{64}$$

This result shows that the pressure at the outer edge of the boundary layer is quite large near the leading edge of the plate, and approaches a constant value as x becomes large.

The pressure at the plate surface is now given by

$$p(x,0) = p_1 + 4\nu(\lambda - 1)\left(\frac{\eta_1 V}{2(1+3\lambda)\nu x}\right)^{1/3} . \tag{65}$$

The pressure at the plate is once again less than the pressure at the outer edge of the boundary layer, which in turn is higher than the far field pressure p_1. If $\lambda > 1$, "ridging" occurs throughout the boundary layer. The highest portion of the ridge occurs at the outer edge of the boundary where there is a rather abrupt return to the level of the plastic region along the yield boundary. Considering the thinness of the boundary layer itself it would appear that the nonuniform stressing of the elastic portion of the ice-water field would probably cause the ridging to be confined to a narrow region adjacent to the plate as expected.

It is also noted that in this case that the drag has a modest velocity dependence as well as a minimum value for incipient motion. This is, of course, a somewhat more realistic result from an intuitive point of view.

Conclusions and Recommendations

1. A search of the existing literature on ice-water suspensions indicates that the rheology of such suspensions has not been investigated. A useful characterization of highly concentrated broken ice flow fields cannot be accomplished until this is done.

2. In the absence of a rheological description of broken ice fields it is hypothesized that these fields will behave as a Bingham plastic, at least for some range of shear rates near zero. This hypothesis is based on the examination of analogous flow fields.

3. The theoretical basis of two-dimensional Bingham plastic flows is found to be well established and could be used to determine the drag on a ship hull in a concentrated broken ice field. The complexity of the rheological model and the flow field geometry indicate that the only practical way to carry out such an investigation would be to use a computer.

4. The analytical solution of the slow flow around a flat plate for a Bingham plastic reveals a mechanism whereby a "sticking effect" between the ice-water suspension and the hull can be explained.

5. The flat plate boundary layer solution also yields a hydrostatic pressure variation within the boundary layer which can be used to explain the phenomena of "ridging" near the solid surface.

6. The fact that the quantitative results of the flat plate boundary layer analysis are qualitatively in reasonable agreement with observations indicates that the Bingham plastic model warrants further consideration as the rheological model for ice-water suspension flows. What remains to be done is to determine the material coefficients η_b and ν and to apply the two-dimensional equations to more realistic geometries.

REFERENCES

1. Karnis, A., H.L. Goldsmith and S.G. Mason, Can. J. Chem. Engng., 44, 181-193.

2. Karnis, A., H.L. Goldsmith and S.G. Mason, Nature, 200, 159-160.

3. Happel, J. and H. Brenner, Low Reynolds Number Hydrodynamics, Prentice Hall, p.463.

4. Botterill, J.S. and M. vander Kilk, "The Flow Properties of Fluidized Solids," A.I.Ch.E. Symposium Series, No.116, Vol.67, pp.70-76.

5. Milano, V.R., "Ship Resistance to Continuous Motion in Ice," Ph.D. Thesis, Steven Inst. Tech., 1972.

6. Kashteljan, I.I. Poznjak and A.J. Ryvlin, "Ice Resistance to Motion of a Ship," Sudostroenie, Leningrad, 1968.

7. Schürgerl, K., "Rheological Behavior of Fluidized Systems," Chapt.6, p.261, Fluidization, Davidson & Harrison, Ed., Academic Press.

8. Oldroyd, J.G., "A Rational Formulation of the Equations of Plastic Flow for a Bingham Plastic," Proc. Camb. Phil. Soc., Vol.43, p.100, 1947.

9. Oldroyd, J.G., "Two-Dimensional Plastic Flow of a Bingham Solid, A Plastic Boundary Layer Theory for Slow Motion," Proc. Camb. Phil. Soc., Vol.43, p.383, 1947.

NOMENCLATURE

d = characteristic length

e_{ij} = component of strain rate tensor

K = bulk modulus

ℓ = plate length

p, p_1 = pressure

p_{ik} = component of the stress tensor

u_i = component of strain

u, v = velocity components

V = plate velocity

x, y = coordinates

δ = boundary layer thickness

Δ = dilatation

ϵ_{ik} = component of strain tensor

η = apparent viscosity

η_1 = reciprocal mobility

λ = constant

μ = modulus of rigidity

ν = yield value

ψ = stream function